

Electronic Supplementary Information

A tunable bifunctional hollow $\text{Co}_3\text{O}_4/\text{MO}_3$ (M=Mo,W) mixed-metal oxide nanozyme for sensing H_2O_2 and screening acetylcholinesterase activity and its inhibitor

Xiaodan Zhang, Yuwan Lu, Qiumeng Chen, Yuming Huang*

College of Chemistry and Chemical Engineering, Southwest University, Chongqing
400715, China

*Corresponding author. E-mail: ymhuang@swu.edu.cn

Synthesis of ZIF-67

ZIF-67 was prepared as the typical method [1] as follows: 0.582 g of $\text{Co}(\text{NO}_3)_2 \cdot 6\text{H}_2\text{O}$ and 0.656 g of 2-MIM were dissolved in 50 mL methanol to form solution A and B, respectively. Then, the solution B was rapidly poured into solution A under vigorous stirring for 10 min. Finally, the mixture was stand for 24 h at room temperature. After washing with methanol several times, the purple solid powder was collected by centrifugation and dried at 60 °C.

Characterization

The optical absorption was determined on a U-4100 UV-vis-NIR spectrophotometer (Hitachi, Japan). The morphologies of samples were acquired on an S-4800 field emission SEM (Hitachi, Japan) with an accelerating voltage of 25 kV. The TEM images were recorded with a JEM-2100F field emission transmission electron microscopy (JEOL, Japan) at an accelerating voltage of 200 kV. XPS analysis was performed by a ThermoFisher ESCALAB 250Xi spectrometer (Thermo Fisher Scientific, America) and XPS PeakFit software was used for peak fitting of XPS spectra. XRD patterns of the products were determined by a Bruker D8 Advance powder X-ray diffractometer (Bruker, Germany). Mettler Toledo FE20 pH meter (Mettler-Toledo Instruments Co. Ltd., China) was applied for pH value assay. N_2 adsorption-desorption isotherm data were measured on an ASAP 2020 Micromeritics instrument (Maie, USA) at 77 K.

Calculation of the inhibition efficiency

The inhibition efficiency (IE%) of AChE activity was calculated by the following equation:

$$\text{IE}\% = (A_{\text{inhibitor}} - A_{\text{without inhibitor}}) / (A_0 - A_{\text{without inhibitor}}) \times 100\%$$

where $A_{\text{inhibitor}}$ and $A_{\text{without inhibitor}}$ were the absorbance at 652 nm of TMB- H_2O_2 -

Co₃O₄/MoO₃-ATCh/AChE system in the presence and absence of nesotigmine, respectively, and A_0 was the blank absorbance at 652 nm of TMB-H₂O₂-Co₃O₄/MoO₃-ATCh system.

Table S1. The atomic percentage of Co, Mo, W and O elements from XPS results in different products.

Sample	Co	Mo	W	O
Co ₃ O ₄	16.2%	–	–	43.9%
Co ₃ O ₄ /MoO ₃	11.8%	4.5%	–	51.2%
Co ₃ O ₄ /WO ₃	11.3%	–	3.6%	50.4%

Table S2. The peak area ratio of Co and O_{vac} in different samples from XPS analysis.

Sample	Co ²⁺ /Co _{total}	Co ³⁺ /Co _{total}	Co ²⁺ /Co ³⁺	O _{vac} /O _{total}
Co ₃ O ₄	0.45	0.55	0.82	0.24
Co ₃ O ₄ /MoO ₃	0.51	0.49	1.04	0.44
Co ₃ O ₄ /WO ₃	0.76	0.24	3.17	0.46

Table S3. Reproducibility of response for 0.2 mM H₂O₂ among three batches of the as-prepared Co₃O₄/MoO₃ using the same preparation method.

Batch No.	1	2	3
Relative activity (%) ^a	100 ± 3.3	98.5 ± 6.5	94.2 ± 1.6
RSD (%)	1.78		

^a Relative standard deviation (RSD) for three duplicate determinations.

Table S4. Comparison of different methods for AChE detection.

Method	Chemicals	Linear range (U/L)	LOD (U/L)	Ref.
Fluorimetry	Au NCs	0.8 – 12	0.4	[2]
Fluorimetry	carbon QDs	0.05 – 2.0	0.05	[3]
Fluorimetry	C ₃ N ₄ nanodots	0.01 – 3	0.01	[4]
Colorimetry	TMB–ATCh–H ₂ O ₂	2.0 – 14	0.5	[5]
Colorimetry	TMB–MnO ₂ nanosheets	0.1 – 15	0.035	[6]
Colorimetry	TMB–CoOOH nanoflakes	0.05 – 5	0.033	[7]
Colorimetry	TMB–MnOOH nanowire	0.01 – 1.25	0.007	[8]
Colorimetry	TMB–Ag ⁺	0 – 0.03	0.0043	[9]
Colorimetry	Fe-N-C Sazymes-TMB	0.1 – 25	0.014	[10]
Colorimetry	TMB-H ₂ O ₂ -Co ₃ O ₄ /MoO ₃	0.005 – 1.0	0.001	This work

Table S5. The results of neostigmine determination in the water samples

Samples*	Spiked (nM)	Found (nM)	Recovery (%)	RSD (%, <i>n</i> = 3)
Tap water	1	1.03	102.8	3.42
	6	6.08	101.4	4.30
	12	11.84	98.7	3.14
Jialing River water	1	0.96	95.5	1.03
	6	6.01	100.2	3.19
	12	11.71	97.6	1.42

* Tap water and river water samples were collected from our laboratory and Jialing River in Beibei (China, Chongqing), respectively.

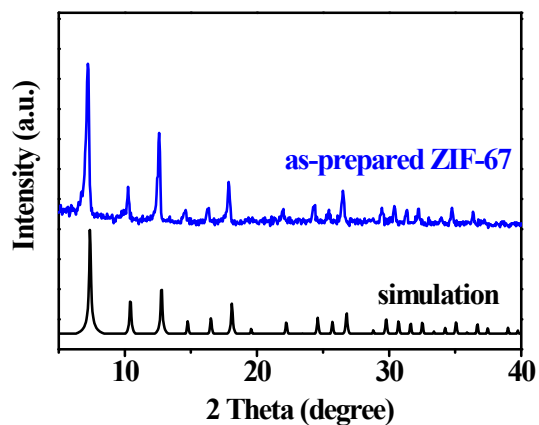


Fig. S1. XRD patterns of ZIF-67.

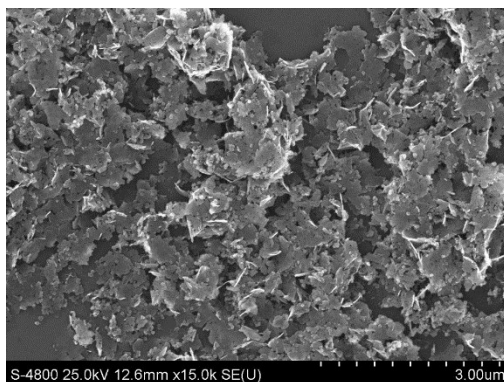


Fig. S2. SEM of Co_3O_4 nanoflakes derived from ZIF-67 without Mo or W-doping.

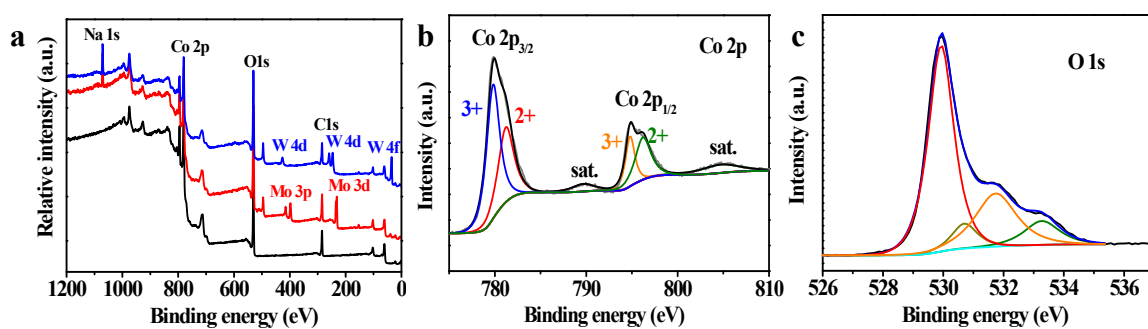


Fig. S3. The full range XPS spectra of Co_3O_4 (black curve), $\text{Co}_3\text{O}_4/\text{MoO}_3$ (red curve) and $\text{Co}_3\text{O}_4/\text{WO}_3$ (blue curve) (a). XPS spectra of the Co 2p (b) and O 1s (c) in pure Co_3O_4 .

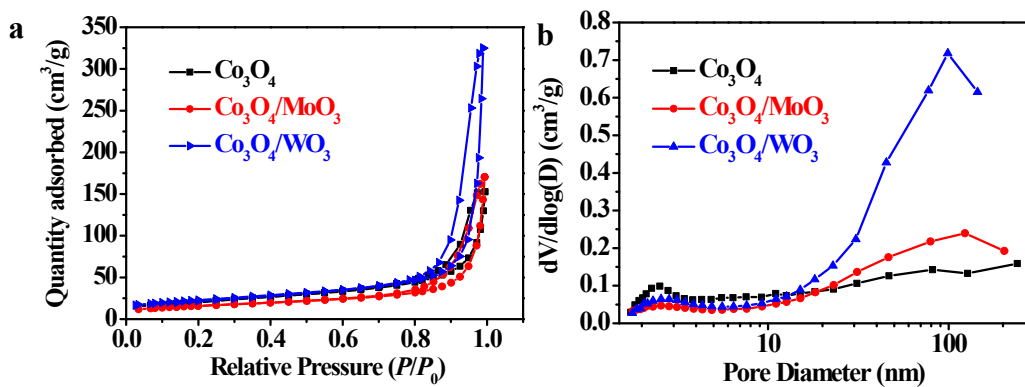


Fig. S4. N_2 adsorption-desorption isotherms of Co_3O_4 , Co_3O_4/MoO_3 and Co_3O_4/WO_3 (a) and their corresponding pore size distribution (b).

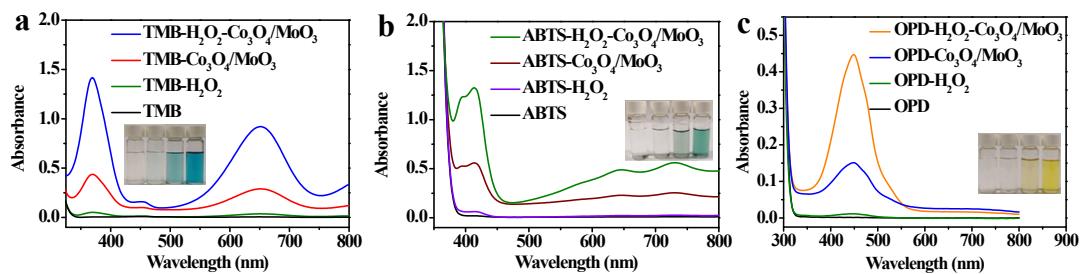


Fig. S5. UV-vis absorption spectra of Co_3O_4/MoO_3 mediated TMB (a) ABTS (b) and OPD (c) colorimetric reactions (Insets show the corresponding solution photos). Conditions: 0.1 mM TMB, 0.5 mM ABTS, 1 mM OPD, 15 mg/L Co_3O_4/MoO_3 , 0.2 mM H_2O_2 , 30 °C, 20 min.

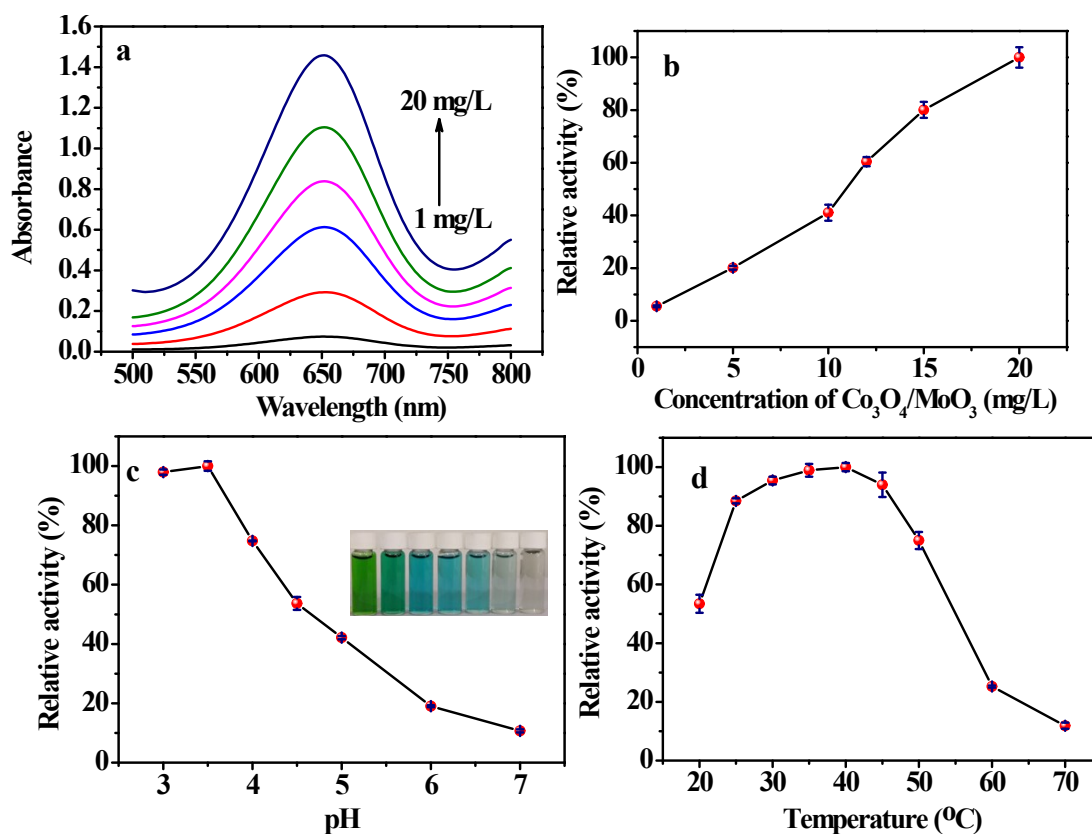


Fig. S6. UV-vis absorption spectra of TMB- H_2O_2 system in the presence of different $\text{Co}_3\text{O}_4/\text{MoO}_3$ concentrations (a) and the relative result (b) (Conditions: 0.1 mM of TMB, 0.2 M NaAc-HAc buffer (pH=4), 30 $^{\circ}\text{C}$, 20 min); effects of pH (c) (Conditions: 0.1 mM of TMB, 12 mg/L of $\text{Co}_3\text{O}_4/\text{MoO}_3$, 30 $^{\circ}\text{C}$, 20 min) and reaction temperature (d) on the peroxidase-like activity of $\text{Co}_3\text{O}_4/\text{MoO}_3$ (Conditions: 0.1 mM of TMB, 12 mg/L of $\text{Co}_3\text{O}_4/\text{MoO}_3$, 0.2 M NaAc-HAc buffer (pH=3.5), 20 min). Inset in Fig. c shows the corresponding photos of solution at different pH (3 to 7, from left to right).

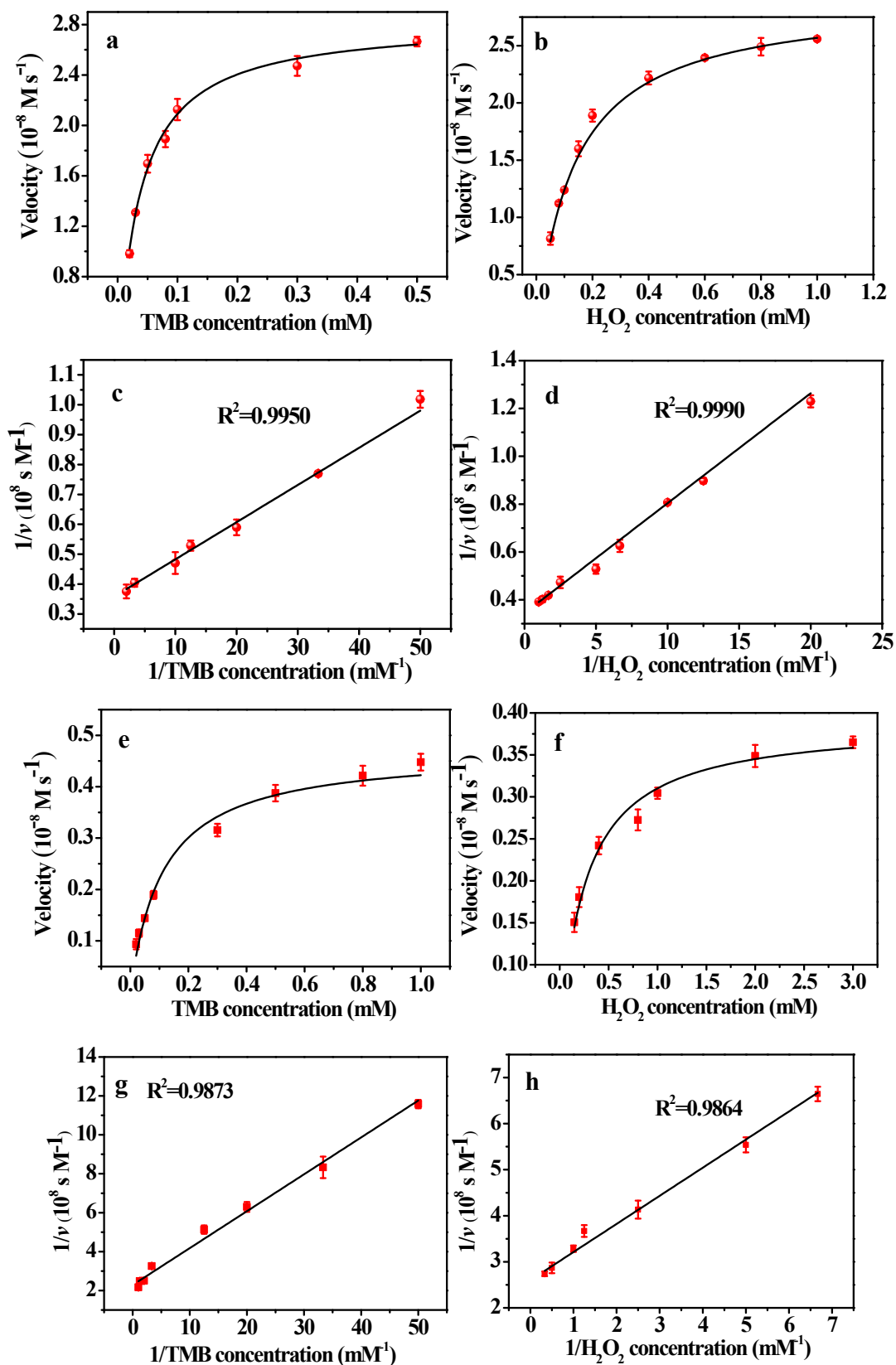


Fig. S7. Steady-state kinetic assay of $\text{Co}_3\text{O}_4/\text{MoO}_3$ and Co_3O_4 . Michaelis-Menten curves for TMB (a) and H_2O_2 (b) of $\text{Co}_3\text{O}_4/\text{MoO}_3$, and the corresponding Lineweaver-Burk plots for TMB (c) and H_2O_2 (d). Michaelis-Menten curves for TMB (e) and H_2O_2 (f) of Co_3O_4 , and the corresponding Lineweaver-Burk plots for TMB (g) and H_2O_2 (h).

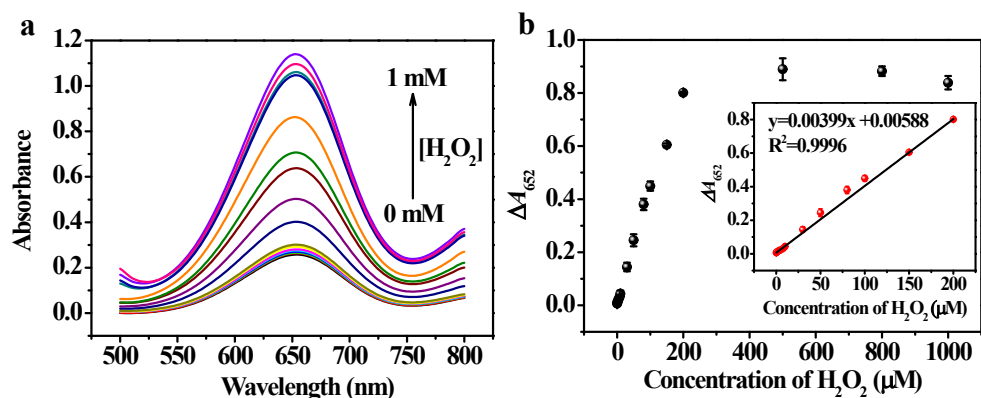


Fig. S8. (a) UV-vis absorption spectra of TMB- $\text{Co}_3\text{O}_4/\text{MoO}_3\text{-H}_2\text{O}_2$ system in the presence of different H_2O_2 concentrations (0, 0.1 μM , 0.5 μM , 1 μM , 3 μM , 5 μM , 8 μM , 10 μM , 30 μM , 50 μM , 80 μM , 100 μM , 150 μM , 200 μM , 500 μM , 800 μM and 1 mM, respectively). (b) Plot of ΔA_{652} versus H_2O_2 concentrations. Inset shows the corresponding linear calibration curve. The error bars represent the standard deviation of three replicate assays. The net absorption intensity ($\Delta A = A_i - A_0$, where A_i and A_0 were the absorbance at 652 nm in the presence and absence of H_2O_2 , respectively).

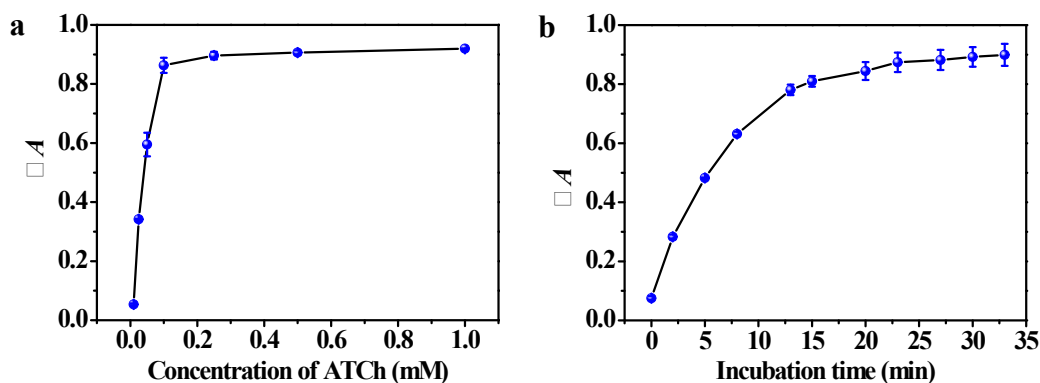


Fig. S9. (a) Effect of ATCh concentration on ΔA of the TMB- $\text{Co}_3\text{O}_4/\text{MoO}_3\text{-H}_2\text{O}_2$ system in the presence of 1 U/L AChE. (b) Effect of incubation time on ΔA of the TMB- $\text{Co}_3\text{O}_4/\text{MoO}_3\text{-H}_2\text{O}_2\text{-ATCh}$ system in the presence of 1 U/L AChE. The inhibitory absorption intensity ΔA denotes $A_0 - A_e$, where A_0 and A_e were the absorbance at 652 nm in the absence and presence of 1 U/L of AChE, respectively.

References

1. F. L. Lyu, Y. C. Bai, Z. W. Li, W. J. Xu, Q. F. Wang, J. Mao, L. Wang, X. W. Zhang and Y. D. Yin, *Adv. Funct. Mater.*, 2017, **27**, 1702324.
2. C. Y. Ke, Y. T. Wu and W. L. Tseng, *Biosens. Bioelectron.*, 2015, **69**, 46-53.
3. W. H. Li, W. Li, Y. F. Hu, Y. L. Xia, Q. P. Shen, Z. Nie, Y. Huang and S. Z. Yao, *Biosens. Bioelectron.*, 2013, **47**, 345-349.
4. M. C. Rong, X. H. Song, T. T. Zhao, Q. H. Yao, Y. R. Wang and X. Chen, *J. Mater. Chem. C*, 2015, **3**, 10916-10924.
5. T. Han and G. F. Wang, *J. Mater. Chem. B*, 2019, **7**, 2613-2618.
6. X. Yan, Y. Song, X. L. Wu, C. Z. Zhu, X. G. Su, D. Du and Y. H. Lin, *Nanoscale*, 2017, **9**, 2317-2323.
7. R. Jin, Z. H. Xing, D. S. Kong, X. Yan, F. M. Liu, Y. Gao, P. Sun, X. S. Liang and G. Y. Lu, *J. Mater. Chem. B*, 2019, **7**, 1230-1237.
8. L. J. Huang, D. W. Sun, H. B. Pu, Q. Y. Wei, L. P. Luo and J. L. Wang, *Sens. Actuat. B*, 2019, **290**, 573-580.
9. P. J. Ni, Y. J. Sun, H. C. Dai, S. Jiang, W. D. Lu, Y. L. Wang, Z. Li and Z. Li, *Sens. Actuat. B*, 2016, **226**, 104-109.
10. Y. Wu, L. Jiao, X. Luo, W. Q. Xu, X. Q. Wei, H. J. Wang, H. Y. Yan, W. L. Gu, B. Z. Xu, D. Du, Y. H. Lin and C. Z. Zhu, *Small*, 2019, **15**, 1903108.